Influence of Initial Wave Steepness of Modulated Wave Trains on the Maximum Crest Height

by Hidetaka Houtani[1], Takuji Waseda[2] and Hiroshi Sawada[3]
[1]School of Engineering, the University of Tokyo, Tokyo, Japan
[2] Graduate School of Frontier Sciences, the University of Tokyo, Chiba, Japan
[3]National Maritime Research Institute, Tokyo, Japan
E-mail: *houtani@sys.t.u-tokyo.ac.jp*

1 INTRODUCTION

Nonlinear quasi-resonant interaction plays a vital role in generating freak waves. Such nonlinear wave evolution is governed by the balance between nonlinearity and dispersion, expressed by a ratio of the wave steepness and spectral bandwidth (e.g., the Benjamin-Feir index for irregular waves [1] and $\hat{\delta}$ for modulated wave trains [2]). In the present study, we performed a numerical simulation using the higher-order spectral method [3] and a corresponding tank experiment that focused on modulated wave trains. Therein, the initial wave steepness was varied, while the spectral bandwidth was fixed. We investigated the influence of the initial wave steepness on the maximum crest height as a consequence of the nonlinear wave evolution. The physics behind the crest height amplification is discussed from spectral-broadening and phase-convergence perspectives.

2 FACILITY AND METHODS

2.1 Numerical Simulations

We numerically simulated the temporal evolution of spatially periodic modulated wave trains using the higher-order spectral method (HOSM) [3]. HOSM solves Laplace's equation ($\nabla^2\phi = 0$) numerically subject to nonlinear kinematic and dynamic free surface boundary conditions. A three-wave system composed of a carrier, upper sideband, and lower sideband waves (denoted as $c, +, -$, respectively) was given as an initial wave profile of the HOSM simulation:

$$\zeta(x) = a_c \cos(k_c x) + a_+ \cos(k_+ x + \varphi_+) + a_- \cos(k_- x + \varphi_-). \quad (1)$$

Here, a, k, φ denote the wave amplitude, wavenumber, and phase, respectively. $k_\pm$ is defined as $k_c \pm \delta k$ where δk is the perturbation wavenumber. We set the carrier wavelength $\lambda_c (= 2\pi/k_c)$ to 3 m, the perturbation wavenumber $\delta k/k_c$ to 1/7, the carrier wave amplitudes $a_\pm/a_0$ to 0.1 with $a_0 = (a_c^2 + a_+^2 + a_-^2)^{1/2}$, and the sideband phases $\varphi_\pm$ to $-\pi/4$, respectively. a_0 expresses the initial amplitude of the Stokes wave. In the simulation, we swept the initial wave steepness $a_0 k_c$ between 0.08 and 0.115 to determine its influence on the maximum crest height.

2.2 Tank Experiment

A wave generation experiment was performed in a wave tank (WT) (50 m × 8 m × 4.5 m) at the National Maritime Research Institute to validate the HOSM simulation and investigate the modulated wave trains, including wave breaking phenomena. We generated the modulated wave trains using the HOSM-WG method [4]. A nonlinear wave field precomputed by HOSM is generated in a wave tank by sending a temporally evolving signal that is calculated based on the HOSM output to a wave-maker. Moreover, HOSM-WG can control when and where the maximum crest height appears in a wave tank. In the present study, we generated the modulated wave trains such that the maximum crest appeared at $t = 40$ s after the beginning of the wave generation and at $x =$12 m from the wave-maker in the WT.

However, the location of the maximum crest can deviate from $x =$12 m, especially when wave-breaking occurs. To measure the maximum crest height (even in cases of wave-breaking), we measured the wave surface using a stereo imaging method [5]. About 100 sphere floats with a diameter of less than 20 mm were set on the wave surface and two cameras tracked the three-dimensional motion of these floats. The wave profiles were estimated from the positions of the floats. The estimation error in the crest height of regular waves with a wavelength of 3 m and wave heights between 10 and 20 cm by this stereo imaging scheme is less than 4% [5]. Note that the standard deviation of the wave-maker motion was found to be 1.065 times larger than the given signal due to a mechanical wave-maker control problem. Therefore, the initial wave steepness $a_0 k_c$ for the experimental results presented in Section 3 were corrected by multiplying it by 1.065.

3 RESULTS OF NUMERICAL SIMULATIONS AND EXPERIMENTS

In this section, we compare the maximum crest height of the modulated wave trains obtained from the HOSM simulation and the HOSM-WG experiment in the WT. The variation of the normalized maximum crest height ζ_{cr}/a_0 with the initial wave steepness $a_0 k_c$ is presented in Fig. 1. The Akhmediev breather (AB) solution of the nonlinear Schrödinger equation [6] is also presented as a reference in Fig. 1. Overall, ζ_{cr}/a_0 increases with $a_0 k_c$, but the HOSM simulation and WT experiment results are notably larger than the AB prediction. For lower a_0k_c, the HOSM and WT results agree well ($a_0k_c < 0.106$). However, at larger a_0k_c, a_0k_c continues to increase in the HOSM result, and begins to decrease in the WT result ($a_0k_c > 0.109$). This deviation can be attributed to a stronger nonlinearity in the WT experiment as follows. Wave breakings were found in the WT experiment for $a_0k_c > 0.108$, although a wave breaking could not be reproduced in the HOSM simulation. This stronger nonlinearity led to a higher crest height around $a_0k_c = 0.108$. However, the maximum crest height ζ_{cr}/a_0 decreased with a_0k_c beyond the breaking/non-breaking margin ($a_0k_c = 0.108$) because larger wave breakings were found to occurr during an earlier stage prior to the peak of the modulation. However, we should note that a satisfactory agreement between HOSM and WT results for $a_0k_c < 0.106$ validate the HOSM simulation in the non-breaking regime.

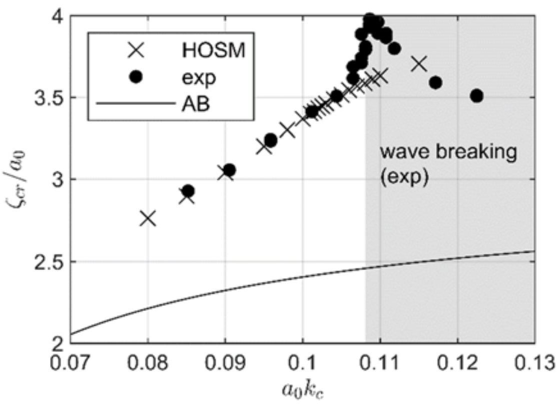

Fig. 1 Variation of the maximum crest height with the initial wave steepness. AB (solid curve) denotes the Akhmediev breather solution of the nonlinear Schrödinger equation.

4 DISCUSSIONS

4.1 Spectral Broadening and its Influence on Maximum Crest Height

In Section 3 we describe that the maximum crest height of the modulated wave trains were found to be much larger in the HOSM simulation and HOSM-WG experiment than in the AB prediction. This difference implies the influence of bound waves and spectral broadenings. This is because the HOSM simulation includes bound wave components and does not restrict the spectral shape, while the AB is a free wave solution and assumes a narrow-banded spectrum. Therefore, in this section, we discuss the influence of the spectral broadenings on the maximum crest height. Herein, the contributions of the free and bound components are separately analyzed.

The spectrum of the modulated wave train varies during its nonlinear evolution. Gibson and Swan (2007) [7] introduced the “amplitude sum” as an indicator of such a spectral broadening:

$$A_s = \sum_j \left|\hat{\zeta}(k_j)\right|. \tag{2}$$

Here, $\hat{\zeta}(k)$ denotes a complex Fourier amplitude of a wave train in the wavenumber space. A_s expresses the potential maximum of the crest height achieved when all the component waves are in-phase. In a system in which the total wave energy $\left(E = \sum_j \left|\hat{\zeta}(k_j)\right|^2\right)$ conserves, A_s increases as the spectrum becomes more broad-banded [7]. Therefore, by evaluating A_s from the HOSM output, we investigate here the influence of the initial wave steepness on spectral broadening and the resultant potential maximum of the crest height. In the analysis, we applied an ideal filter to the wavenumber-frequency spectrum of the HOSM output to separate free and bound components (see [4]) and investigated the bound wave contribution to the crest height.

The relationship between the initial wave steepness a_0k_c and the amplitude sum A_s is presented in Fig. 2. A_s/a_0 increases as a_0k_c becomes larger. Furthermore, the contribution of the bound waves to A_s becomes larger as a_0k_c increases. Specifically, the bound-wave contribution to A_s increases from 8.9 % for $a_0k_c = 0.08$ to 27 % for $a_0k_c = 0.115$. This result indicates that the broadening of the free wave spectrum, due to the increase of a_0k_c, energizes the bound wave production.

Thus far, we have discussed the spectral broadening using A_s. However, the meaning of A_s with regards to the spectral broadening seems to be indirect. Accordingly, we will confirm the spectral broadening with a_0k_c using another parameter ΔK defined as the mean wavenumber difference ($\Delta k = k - k_c$) from the carrier wavenumber weighted by the Fourier amplitude [8]:

$$\Delta K = \left|\frac{\sum_j \Delta k_j^2 \left|\hat{\zeta}(k_j)\right|^2}{\sum_j \left|\hat{\zeta}(k_j)\right|^2}\right|^{1/2}, \quad \text{with} \quad \Delta k_j = k_j - k_c. \tag{3}$$

From the relation between a_0k_c and ΔK (Fig. 3), the spectral broadening according to the increase of the initial wave steepness is confirmed.

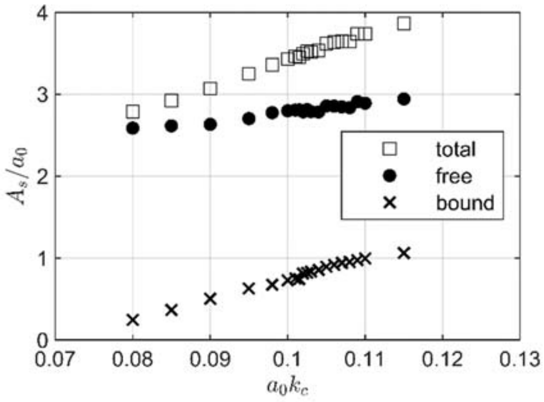

Fig. 2 Relation between the initial wave steepness and amplitude sum of the modulated wave trains.

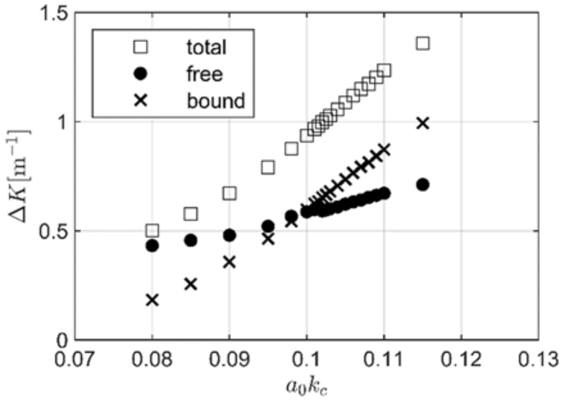

Fig. 3 Relation between the initial wave steepness and mean wavenumber difference of the modulated wave train.

4.2 Phase-Convergence During a Nonlinear Evolution of a Modulated Wave Train

In section 4.1, we revealed that the potential maximum of the crest height of the modulated wave train increased as the initial wave steepness increased. However, this result does not necessarily indicate an increase of the maximum crest height. The convergence of the component wave's phases is necessary to achieve the crest height ζ_{cr} close to its potential maximum A_s. Therefore, in this section, we investigate the degree of phase-convergence at the location and instance of the maximum crest height using the HOSM output. Here, we define x_f and t_f as the location and time of the maximum crest height, respectively. Thus, the maximum crest height can be shown as:

$$\zeta_{cr} = \zeta(x_f, t_f) = \sum_j \mathrm{Re}\left[\alpha(k_j)\right] \quad \text{with} \quad \alpha(k_j) \equiv \hat{\zeta}(k_j, t_f)\exp(ik_j x_f). \tag{4}$$

The modulus and argument of α_j express the Fourier amplitude and phase of the component waves at the location and instance of the maximum crest height, respectively. An example of the amplitude and phase of the component waves for $a_0k_c = 0.105$ is presented in Fig. 4. Many component waves are in-phase at 0. The phases of some components with lower and higher wavenumbers ($k < 1\ \mathrm{m}^{-1}$ and $k > 7.5\ \mathrm{m}^{-1}$) are not necessarily 0. However, the amplitude spectrum (Fig. 4(a)) indicates that the energy of such components is very low.

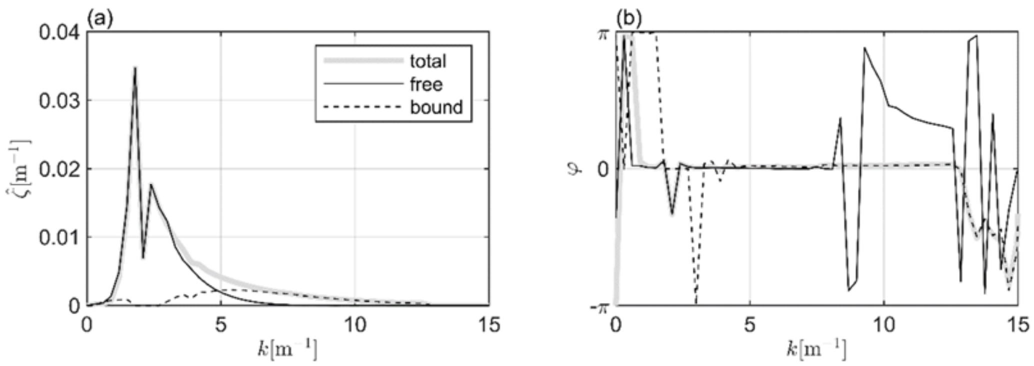

Fig. 4 (a) Amplitude and (b) phase of the component waves of the modulated wave train with $a_0k_c = 0.105$ at the location and timing of the maximum crest height.

To quantify the degree of in-phase, we introduce the following indicator $DOIP$ (degree of in-phase) expressing the ratio between the crest height ζ_{cr} and its potential maximum A_s:

$$DOIP = \frac{\sum_j \mathrm{Re}\left[\alpha(k_j)\right]}{\sum_j \left|\alpha(k_j)\right|}\left(= \frac{\zeta_{cr}}{A_s}\right). \tag{5}$$

$DOIP$ for all the cases with a_0k_c from 0.08 to 0.115 is presented in Fig. 5. $DOIP$ is close to 1 for all the cases, which means that the most components are in-phase at 0. A slight decrease of $DOIP$ for the total (free + bound) wave against

a_0k_c was noted. However, the spectral-broadening contribution (Section 4.1) exceeds the decrease of the phase convergence, and accordingly, the maximum crest height ζ_{cr}/a_0 increases with a_0k_c (Fig. 1).

Note that the $DOIP$ of the bound waves is smaller than that of the free waves (Fig. 5). This small $DOIP$ for the bound waves can be partially attributed to the fact that the phase of a bound wave produced by the interaction between free waves does not necessarily coincide with the phase of these free waves if these free waves are in-phase. For example, the bound wave produced by the interaction of the free waves with $k = k_1$ and k_2 was revealed to be out of phase with these free waves when $k_1/k_2 < 0.296$ [9]. The existence of such out-of-phase bound waves is indicated in the phase spectrum (Fig. 4(b)); the subharmonic bound waves, which are around $k = 1\ \mathrm{m}^{-1}$ ($\varphi \approx \pi$), are out of phase with most of the free waves ($\varphi \approx 0$).

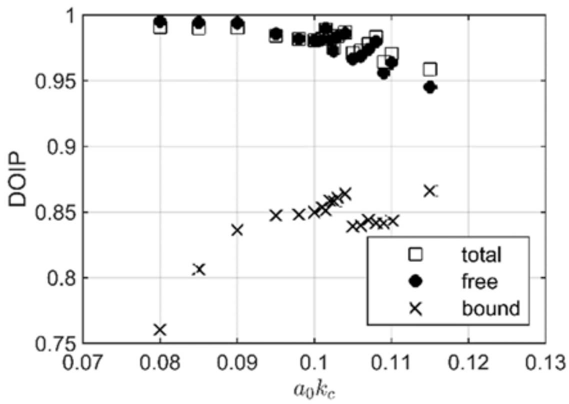

Fig. 5 Relation between the initial wave steepness and degree of in-phase

5 CONCLUSION

We investigated the influence of the initial wave steepness on the maximum crest height of modulated wave trains through tank experiments and HOSM simulations. The study revealed that the maximum crest heigh normalized by the initial amplitude of the Stokes wave ζ_{cr}/a_0 increases with the initial wave steepness a_0k_c if a large wave breaking does not occur. The increase in the initial wave steepness intensifies the quasi-resonant interaction, and accordingly, the spectrum broadens more at its peak modulation. The spectral broadening relates to the potential maximum of the crest height. Furthermore, most of the component waves are in phase at the peak modulation. Accordingly, the crest height is amplified with the initial wave steepness. We should note that a monotonic increase of ζ_{cr}/a_0 with a_0k_c in the non-breaking regime observed in this study is caused by the fixed spectral bandwidth $\delta k/k_c$. The maximum crest height (or wave height) can vary with the spectral bandwidth for a given initial wave steepness [10].

ACKNOWLEDGEMENT

We thank Katsuji Tanizawa for useful discussions.

REFERENCES

[1] Janssen, P. A. (2003). Nonlinear four-wave interactions and freak waves. Journal of Physical Oceanography, 33(4), 863-884.

[2] Tulin, M. P., & Waseda, T. (1999). Laboratory observations of wave group evolution, including breaking effects. Journal of Fluid Mechanics, 378, 197-232.

[3] West, B. J., Brueckner, K. A., Janda, R. S., Milder, D. M., & Milton, R. L. (1987). A new numerical method for surface hydrodynamics. Journal of Geophysical Research: Oceans, 92(C11), 11803-11824.

[4] Houtani, H., Waseda, T., Fujimoto, W., Kiyomatsu, K., & Tanizawa, K. (2018). Generation of a spatially periodic directional wave field in a rectangular wave basin based on higher-order spectral simulation. Ocean Engineering, 169, 428-441.

[5] Houtani, H., Waseda, T., & Tanizawa, K. (2017). Measurement of spatial wave profiles and particle velocities on a wave surface by stereo imaging–validation with unidirectional regular waves. Journal of the Japan Society of Naval Architects and Ocean Engineers, 25, 93-102. (in Japanese)

[6] Akhmediev, N. N., Eleonskii, V. M., & Kulagin, N. E. (1987). Exact first-order solutions of the nonlinear Schrödinger equation. Theoretical and mathematical physics, 72(2), 809-818.

[7] Gibson, R. S., & Swan, C. (2007). The evolution of large ocean waves: the role of local and rapid spectral changes. Proceedings of the Royal Society A: Mathematical, Physical and Engineering Sciences, 463(2077), 21-48.

[8] Thyagaraja, A. (1979). Recurrent motions in certain continuum dynamical systems. The Physics of Fluids, 22(11), 2093-2096.

[9] Houtani, H. (2015). Reproducing freak waves in experimental wave basin (Doctoral dissertation, Ph. D. thesis, The University of Tokyo). UTokyo Repository. (in Japanese)

[10] Waseda, T., Rheem, C. K., Sawamura, J., Yuhara, T., Kinoshita, T., Tanizawa, K., & Tomita, H. (2005, January). Extreme wave generation in laboratory wave tank. In The Fifteenth International Offshore and Polar Engineering Conference. International Society of Offshore and Polar Engineers.